The binding of atomic hydrogen on graphene from density functional theory and diffusion Monte Carlo calculations

Amanda Dumi,[1] Shiv Upadhyay,[1] Leonardo Bernasconi,[1,2] Hyeondeok Shin,[3] Anouar Benali,[3] and Kenneth D. Jordan[1,4,a)]

[1)] *Department of Chemistry, University of Pittsburgh, Pittsburgh, Pennsylvania 15260, USA*

[2)] *Center for Research Computing, University of Pittsburgh, Pittsburgh, Pennsylvania 15260, USA*

[3)] *Computational Science Division, Argonne National Laboratory, Argonne, Illinois 60439, USA*

[4)] *Department of Chemical and Petroleum Engineering, University of Pittsburgh, Pittsburgh, Pennsylvania 15260, USA*

(Dated: 1 September 2022)

In this work density functional theory (DFT) and diffusion Monte Carlo (DMC) methods are used to calculate the binding energy of a H atom chemisorbed on the graphene surface. The DMC value of the binding energy is about 16% smaller in magnitude than the Perdew-Burke-Ernzerhof (PBE) result. The inclusion of exact exchange through the use of the Heyd–Scuseria–Ernzerhof (HSE) functional brings the DFT value of the binding energy closer in line with the DMC result. It is also found that there are significant differences in the charge distributions determined using PBE and DMC approaches.

I. INTRODUCTION

The unique electronic, optical, and transport properties of graphene make it an important system for a wide range of applications, many of which involve or are impacted by the adsorption of atoms or molecules. To bring these applications to fruition, a deeper understanding of the interaction of atoms and molecules with graphene is required, and, not surprisingly, this has been the subject of several experimental and theoretical studies.[1–13]

The adsorption of H atoms on graphene has been the subject of multiple studies.[3,10–14] It is known that there is both a weakly absorbed state in which barriers for diffusion are small and a much more strongly bound chemisorbed state[15,16] , which is the focus of this work. Chemisorbed H atoms open up the band gap and allow for tuning of electronic properties.[17] It has been demonstrated that even a single chemisorbed hydrogen atom causes an extended magnetic moment in the graphene sheet.[18,19] On the other hand, there is evidence that given the ready diffusion of H in the physisorbed state, the H atoms tend to pair up on the surface leading to non-magnetic species.[20] Finally, interest in the hydrogen/graphene system has also been motivated by the potential use of graphene and graphitic surfaces for hydrogen storage.[9] In spite of the interest in H chemisorbed on graphene, we are unaware of experimental values of the binding energy.

Most computational studies of adsorption of atoms and molecules on graphene have employed density functional theory (DFT), primarily due to its favorable scaling with system size, allowing for the treatment of larger periodic structures. However, a reliable theoretical description of interactions at the graphene surface has proven to be challenging for DFT.[1–3,21] In recent years considerable progress has been made in extending correlated wave function methods to periodic systems.[22–27] Among these methods, the diffusion Monte Carlo (DMC)[28] method, which is a real-space stochastic approach to solving the many-body Schrödinger equation is particularly attractive given its low scaling with the number of electrons and high parallelizability. DMC also has the advantages of being systematically improvable and its energy being much less sensitive to the basis set employed than methods that work in the space of Slater determinants. In DMC calculations, the atomic basis set is important only to the extent that it impacts the nodal surface. DMC has been used to describe the adsorption of various species on graphene including O_2[4], a water molecule[5,29], and a platinum atom.[6] In a study of a physisorbed H atom on graphene, Ma et al. found that different DFT functionals gave binding energies ranging from 5 to 97 meV, while DMC calculations gave a value of only 5 ± 5 meV.[3] Various DFT calculations utilizing the Perdew-Burke-Ernzerhof (PBE)[30] and Perdew-Wang (PW91)[31] functionals predict the chemisorbed H atom species to be bound by 480 to 1,440 meV.[32–40] However, this large spread is primarily a result of some calculations employing small supercells resulting in an unphysical description of the low-coverage situation, too small a k-point grid, or small atom-localized basis sets that do not adequately describe the binding and introduce large basis set superposition error (BSSE). In the present work, we use the DMC method to calculate the binding energy of H to graphene in the chemisorbed state.

[a)] Corresponding author: jordan@pitt.edu

II. METHODS

All calculations reported in this study used a 5x5x1 supercell of graphene, as it was large enough to make inconsequential the interaction between periodic images of the adsorbed hydrogen atom and to assure that there are essentially unperturbed C atoms between the buckled regions in adjacent images in the x and y directions. The geometries of graphene, both pristine and with a chemisorbed H atom, were provided by Kim et al.,[41] and were obtained using the PBE+D3 DFT method.[30,42] For all systems, a vacuum spacing of 16 Å was used.

A. Density functional theory calculations

The single particle orbitals used in the trial wave functions for variational Monte Carlo (VMC) and DMC calculations were calculated using the PBE functional with the correlation consistent electron core potential (ccECP)[43,44] pseudopotentials and a plane wave basis with an energy cutoff of 3,400 eV. Monkhorst-Pack k-point grid meshes[45] were employed with a 13.6 meV Marzari-Vanderbilt-DeVita-Payne cold smearing of the occupations.[46] The PBE results were converged at a 6x6x1 k-point grid to 1 meV for graphene and graphene with an adsorbed hydrogen atom. The hydrogen atom trial was generated using a 1x1x1 k-point grid. Convergence studies can be found in Table S1 and S2 of the Supplementary Material.

In addition to the PBE calculations used to generate the trial wave functions for DMC, DFT calculations were carried out with the PBE0[47] and Heyd–Scuseria–Ernzerhof (HSE) functionals[48] to determine if inclusion of exact exchange proves important for the adsorption energy. Due to the inclusion of exact exchange, these calculations would be computationally prohibitive in a plane wave basis, particularly with the high energetic cutoff required by the ccECP pseudopotential. For this reason, they were carried out all-electron with the POB-TZVP Gaussian type orbital (GTO) basis set.[49] Due to the use of GTOs, these calculations suffer from basis set superposition error (BSSE), which we corrected using Grimme's geometry-dependent counterpoise correction scheme.[50,51] This correction resulted in a 113 meV reduction in the magnitude of the binding energy when using the PBE0 functional. For the PBE0 and HSE calculations, a 12x12x1 k-point grid was used to assure binding energies converged to within 2meV. Convergence data are supplied in Table S3 of the Supplementary Material.

The plane wave DFT calculations were carried out with the QUANTUM ESPRESSO version 6.3 code.[52–54] The Gaussian basis DFT calculations were carried out with CRYSTAL17,[55,56] save for the HSE calculation of the isolated hydrogen atom which was carried out using NWChem version 6.8[57] using the same basis as the calculations in CRYSTAL17.

B. Quantum Monte Carlo calculations

DMC is a projector quantum Monte Carlo (QMC) method, solving the Schrödinger equation in imaginary time $\tau = it$; any initial state $|\psi\rangle$, that is not orthogonal to the true ground state $|\phi_0\rangle$, will evolve to the ground state in the long time limit. When dealing with Fermionic particles, the DMC method requires the use of the fixed-node approximation[58] to maintain the antisymmetric property of the wave function. For efficient sampling and to reduce statistical fluctuations, we use a Slater-Jastrow trial wave function fixing the nodes through a Slater determinant comprised of single-particle orbitals, which, in this work, are expanded in a B-spline basis. The Jastrow factor is a function that reduces the variance by explicitly describing dynamic correlation. The Jastrow factor contains terms for one-body (electron-ion), two-body (electron-electron) and three-body (electron-electron-ion) interactions. The one- and two-body terms were described with spline functions[59], while the three-body terms were represented by polynomials.[60] 10 parameters were used for the one-body terms per atom type, and 10 parameters were employed per spin-channel for the two-body terms. The cutoffs on the one- and two-body terms were fixed to the Wigner-Seitz radius of the simulation cell. The three-body terms were comprised of 26 parameters per term with a cutoff of 10 Bohr. The parameters in the Jastrow factor were separately optimized for each geometry with the linear method[61] using VMC. To reduce the cost of the DMC calculations as well as to reduce the fluctuations near the ionic core regions, ccECP pseudopotentials were used to replace the core electrons.[43,44] The ccECP pseudopotentials were designed to be used with high-accuracy many-body methods. The non-local effects due to the pseudopotentials were addressed using the determinant-localization approximation along with the t-moves method (DLTM).[62,63] Finite size effects were addressed using twist averaging.[64] The twist angles were chosen to be the symmetry unique points of the 6x6x1 k-point grid shifted by half a grid step away from the gamma point in each direction.

The DMC calculations were performed using the branching scheme proposed by Zen et al. (ZSGMA)[65] with a population control target of 8,192 walkers and a time step of 0.005 a.u., which represented a balance between computational cost and finite timestep error in previous work.[66]

We define the binding energy as

$$E_b = E_{dgr+H} - (E_{gr} + E_H) \tag{1}$$

where E_{dgr+H} is the energy of the distorted graphene sheet with a chemisorbed atomic hydrogen, E_H is the energy of a hydrogen atom, and E_{gr} is the energy of a pristine graphene sheet. In the chemisorbed state, the hydrogen atom bonds directly over a carbon atom, causing this carbon to be pulled out of the sheet towards the hydrogen.[67,68] The adjacent carbons are also pulled

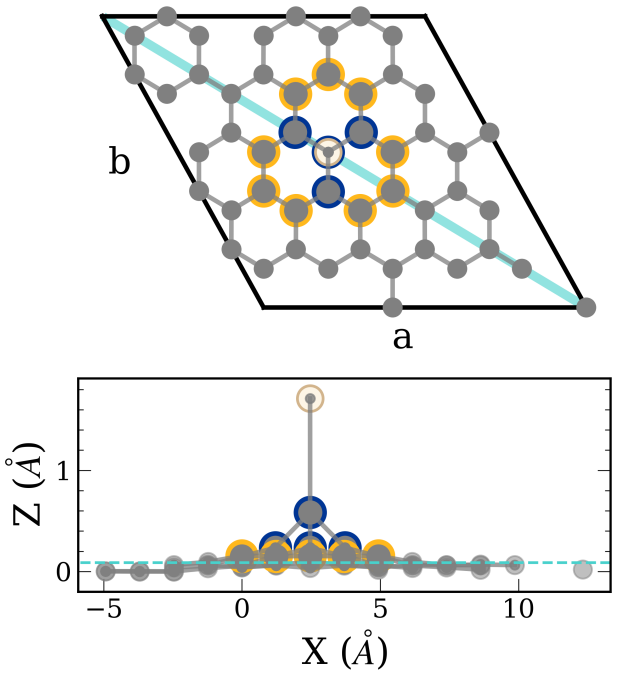

FIG. 1. Perpendicular view of the simulation cell (top) and a parallel view obtained by projection onto the xz-plane (bottom). The carbon atoms are colored gray and the hydrogen atom is denoted as white. For the perpendicular view, the cyan line represents the slice of the cell used to visualized electron density differences. For the parallel view, the dotted cyan line represents the mean carbon z position. Blue outlined atoms are greater than one standard deviation away from the mean carbon z position, whereas yellow atoms are between 0.5-1.0 σ.

in the direction of the hydrogen leading to a distorted graphene sheet.

The QMC calculations were carried out using the QMCPACK code, with the workflow between QUANTUM ESPRESSO and QMCPACK managed by Nexus.[69–71] Figures 1 and 3 were rendered with matplotlib[72] and the density plots were generated using VESTA.[73]

III. RESULTS & DISCUSSION

A. Binding energy

Table I contains a summary of the binding energies of a hydrogen atom chemisorbed on graphene from this work and selected values from previous publications using the PW91 and PBE functionals. These literature values range from -790 to -980 meV. This wide spread of binding energies is caused by (1) the use in some studies of small supercells for which there are sizable interactions between the CH groups in adjacent cells, and (2) the use in some studies of small atom-centered basis sets without corrections for BSSE. Our calculations with the PBE functional in conjunction with a plane wave basis set give a binding energy of -821 meV. This should be contrasted with our -691 ± 19 meV DMC result. There are several possible sources for the difference between the PBE and DMC values of the binding energy. These include errors in the DFT calculations due to self interaction and planar graphene having more multiconfigurational character than H/graphene, with this being better described with DMC than with PBE. We note that the inclusion of the D3 dispersion correction with the PBE functional only changes the magnitude of the binding energy by 0.03 eV.

TABLE I. Binding energy (meV) of a hydrogen atom chemisorbed on graphene calculated with various DFT functionals and with DMC.

Method	Binding energy
This Work	
PBE [a]	-821
PBE[b]	-871
PBE0[b]	-851 (-800)
HSE[b]	-794 (-743)
DMC	-691 ± 19
Previous Work	
PW91	-810 to -830[33], -870[34]
PBE	-790[35], -840[36], -980[37]

[a] Calculation was done in the plane wave basis
[b] Calculation was done in the Gaussian basis set with corrections for BSSE. Values in parentheses include a correction for the basis set incompleteness as described in the text.

The PBE binding energy is 51 meV lower in magnitude in the plane wave than in the GTO basis set when the same k-point grid is used, and this value is used as a correction for the basis set incompleteness error for the results with other functionals in Table I. The calculations in the GTO basis set give a slightly smaller in magnitude binding energy with PBE0 than with PBE. However, with HSE, we obtain a binding energy 77 meV smaller in magnitude than the PBE result. Applying the correction for the basis set incompleteness error, we obtain -800 meV for the PBE0 binding energy and -743 meV for the HSE binding energy, with the latter being in reasonable agreement with the DMC result of -691 meV. Although the 130 meV difference between the plane-wave PBE and DMC values of the binding energy may appear to be small, this energy difference, of that magnitude is consistent with an order of magnitude change in the hydrogen evolution current at room temperature on graphene electrodes.[41]

In order to better understand the origin of the difference in the PBE and HSE H-atom adsorption energies, we also carried out non-self-consistent calculations, using PBE densities to evaluate the HSE energies. These calculations gave a binding energy only 21 meV smaller in magnitude than obtained from the self-consistent HSE calculations. This demonstrates that the functional is more important than the density in establishing the bind-

ing energy. Detailed information can be found in Table S4 of the Supplementary Material.

Detailed results of the DMC calculations can be found in Tables S5-S7 in the Supplementary Material.

B. Binding density

It is instructive to examine the change in the electron density associated with the binding of the H atom to the distorted graphene as determined from the PBE and DMC calculations. The density change is given by

$$\rho_b = \rho_{dgr+H} - (\rho_{dgr} + \rho_H), \quad (2)$$

where ρ_H is the charge density of the hydrogen atom, and ρ_{dgr+H} and ρ_{dgr} are the charge densities of the distorted graphene sheet with and without hydrogen, respectively. For the QMC density, the density was accumulated during the VMC and DMC calculations, the mixed estimator bias was found to be insignificant, and was thus not corrected.

The ρ_b density differences for both DMC and PBE are shown in Figure 2. The dark blue and gold regions represent a loss and gain of electron density, respectively. As expected, there is a shift in electron density from the carbon atom participating in the carbon-hydrogen bond as well as to the three adjacent carbon atoms. These qualitative changes in the density are consistent with previous theoretical and experimental studies.[67,68] The rehybridization from sp^2 to sp^3 of the carbon participating in the CH bond and the weakening of the π bonds due to the distortion of the graphene lead to the electron density shift. The change in the charge distribution is similar for PBE and DMC, with the most noticeable difference being a greater increase of density at remote C atoms in the DMC than in the PBE calculations.

C. Charge density differences between DMC and PBE

In this section, the difference between the DMC and PBE charge densities for distorted graphene with the adsorbed hydrogen atom as well as for pristine planar graphene without the adsorbed hydrogen atom are considered. The charge density difference for each system is calculated according to

$$\Delta\rho_{system} = \rho^{DMC}_{system} - \rho^{PBE}_{system}, \quad (3)$$

where ρ^{DMC}_{system} is the DMC charge density of a given system (either distorted graphene with the adsorbed hydrogen or pristine graphene) and ρ^{PBE}_{system} is the corresponding PBE charge density. $\Delta\rho_{gr}$ and $\Delta\rho_{dgr+H}$ are reported in Figure 3 along the 110 slice through the unit cell, which captures the carbon-hydrogen bond. From the top-down perspective in Figure 1, the 110 lattice plane bisects the cell diagonally through the longer of the two diagonals and is indicated by the solid cyan line. In Figure 3, blue represents areas where the PBE density is larger, while gold areas represent areas where the DMC density is larger. The DMC density, in comparison with the PBE density, has greater weight in the bonding region between atoms. We note that the HSE density displays similar differences as the PBE density. Figure S2 of the Supporting Information includes a visualization of the DMC-HSE density difference. This is the case for both the planar graphene without hydrogen and the system with hydrogen chemisorbed to graphene. Even though there are significant differences between the PBE and DMC densities for both systems, the difference is similar in the two systems, consistent with it not introducing a large error in the PBE value of the binding energy.

IV. CONCLUSIONS

Calculations of the binding energy of a hydrogen atom on a graphene sheet were carried out using various DFT methods and with DMC. The DMC calculations provide a benchmark value of the binding energy.

Our best estimate of the binding energy from DMC calculations is -691 ± 19 meV. The PBE result obtained with a plane-wave basis set gives a binding energy about 20% larger in magnitude than the DMC result. The global hybrid functional, PBE0, gives a binding energy close to that of PBE. In comparison, HSE, a range-separated hybrid functional, gives a smaller binding energy of -743 meV, after a correction applied for the basis set incompleteness error, and is much closer to the value from DMC calculations. Interestingly, there are significant differences in the DMC and PBE charge densities of both graphene and H/graphene.

SUPPLEMENTARY MATERIAL

The supplementary material document includes the total energies and error bars for the quantum Monte Carlo calculations, the total energies for the DFT calculations, and details of the convergence of the DFT total energies with respect to the k-point grid and kinetic energy cutoff of the plane wave basis, and a comparison of the density difference of DMC-PBE and DMC-HSE.

ACKNOWLEDGEMENTS

We thank Dr. Dan Sorescu for helpful discussion and for sharing the coordinates of his calculations. A.B. and H.S were supported by the U.S. Department of Energy, Office of Science, Basic Energy Sciences, Materials Sciences and Engineering Division, as part of the Computational Materials Sciences Program and Center for Predictive Simulation of Functional Materials. An award of computer time was provided by the Innovative and Novel

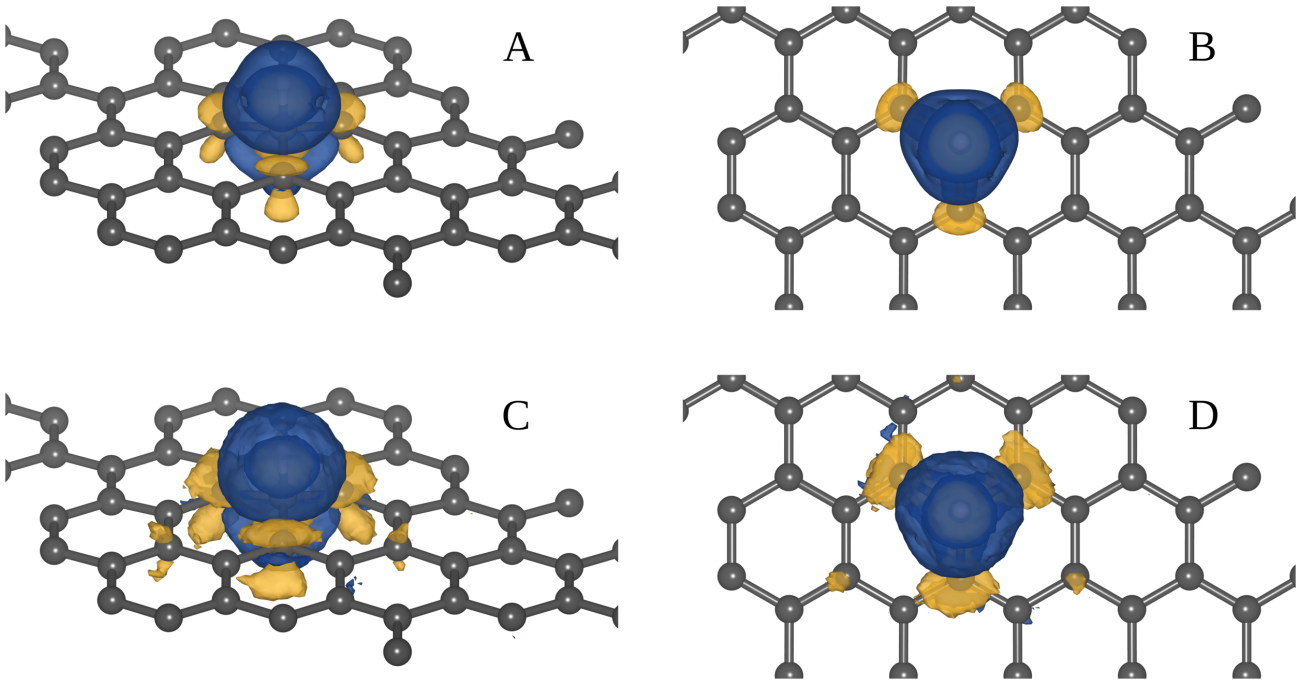

FIG. 2. Change of the electron density due to the adsorption of the H atom to the distorted graphene sheet (Eq. 2). ρ_b from PBE calculations is shown from an oblique angle (A) and aligned along the c axis (B). ρ_b from DMC calculations (C) and (D) is shown from the same perspectives. Gold and blue represent a gain and loss of electron density, respectively. Note that there is a region of increased charge density at the C-H bond that is enveloped by a region of loss in the charge density. The binding density was visualized using an isovalue of 2.8×10^{-5} for DMC and 3.9×10^{-5} for PBE, in both cases capturing 95% of the differential charge density.

Computational Impact on Theory and Experiment (INCITE) program. The DMC and plane wave DFT calculations used resources of the Argonne Leadership Computing Facility, which is a DOE Office of Science User Facility supported under contract DE-AC02-06CH11357. The DFT calculation using Gaussian orbitals were carried out on computing resources in the University of Pittsburgh's Center for Research Computing. K.D.J. acknowledges NSF (CBET-2028826) for partial support of this work. S.U. was supported in part by the Pittsburgh Quantum Institute (PQI) Graduate Quantum Leader Award.

DATA AVAILABILITY STATEMENT

The data that support the findings of this study are openly available on the Materials Database Facility at `https://acdc.alcf.anl.gov/mdf/detail/dumi_dmc_hgraphene_v1.3`, with the following DOI: 10.18126/s1wc-tya.

[1] T. J. Hughes, R. A. Shaw, and S. P. Russo, "Computational Investigations of Dispersion Interactions between Small Molecules and Graphene-like Flakes," J. Phys. Chem. A **124**, 9552–9561 (2020).
[2] M. Bartolomei, M. I. Hernández, J. Campos-Martínez, R. Hernández-Lamoneda, and G. Giorgi, "Permeation of chemisorbed hydrogen through graphene: A flipping mechanism elucidated," Carbon **178**, 718–727 (2021).
[3] J. Ma, A. Michaelides, and D. Alfè, "Binding of hydrogen on benzene, coronene, and graphene from quantum Monte Carlo calculations," J. Chem. Phys. **134**, 134701 (2011).
[4] H. Shin, Y. Luo, A. Benali, and Y. Kwon, "Diffusion Monte Carlo study of O_2 adsorption on single layer graphene," Phys. Rev. B **100**, 075430 (2019).
[5] J. Ma, A. Michaelides, D. Alfè, L. Schimka, G. Kresse, and E. Wang, "Adsorption and diffusion of water on graphene from first principles," Phys. Rev. B **84**, 033402 (2011).
[6] J. Ahn, I. Hong, G. Lee, H. Shin, A. Benali, and Y. Kwon, "Adsorption of a single pt atom on graphene: spin crossing between physisorbed triplet and chemisorbed singlet states," Phys. Chem. Chem. Phys. **23**, 22147–22154 (2021).
[7] A. K. Geim, "Graphene: Status and Prospects," Science **324**, 1530–1534 (2009).
[8] K. S. Novoselov, A. K. Geim, S. V. Morozov, D. Jiang, M. I. Katsnelson, I. V. Grigorieva, S. V. Dubonos, and A. A. Firsov, "Two-dimensional gas of massless Dirac fermions in graphene," Nature **438**, 197–200 (2005).
[9] O. K. Alekseeva, I. V. Pushkareva, A. S. Pushkarev, and V. N. Fateev, "Graphene and Graphene-Like Materials for Hydrogen Energy," Nanotechnol. Russ. **15**, 273–300 (2020).
[10] S. Niaz, T. Manzoor, and A. H. Pandith, "Hydrogen storage: Materials, methods and perspectives," Renew. Sustain. Energy Rev **50**, 457–469 (2015).
[11] A. Fomkin, A. Pribylov, I. Men'shchikov, A. Shkolin, O. Aksyutin, A. Ishkov, K. Romanov, and E. Khozina, "Adsorption-Based Hydrogen Storage in Activated Carbons and Model Carbon Structures," Reactions **2**, 209–226 (2021).

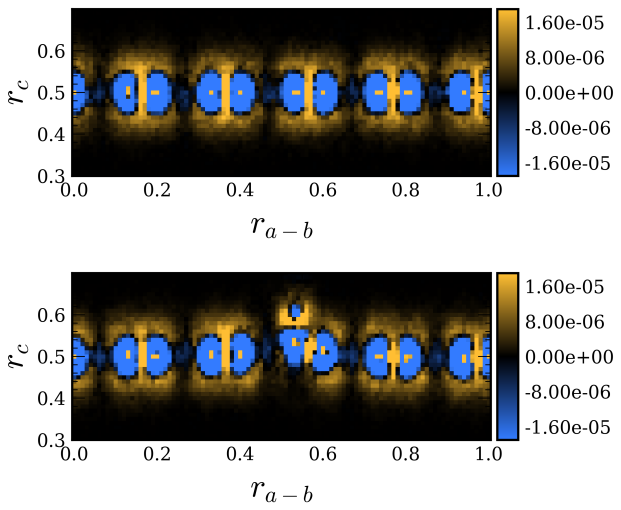

FIG. 3. Visualization of the difference of PBE and DMC densities sliced along the 110 lattice plane of the unit cell for the graphene sheet, $\Delta\rho_{gr}$, (top) and H adsorbed onto graphene, $\Delta\rho_{dgr+H}$, (bottom). The abscissa represents traversing the 110 plane in fractional coordinates, while the ordinate represents traversing the c axis in fractional coordinates. Blue regions represent places where the PBE density is larger, while the gold color represents regions where the DMC density is larger.

[12] C. Ataca, E. Aktürk, S. Ciraci, and H. Ustunel, "High-capacity hydrogen storage by metallized graphene," Appl. Phys. Lett. **93**, 043123 (2008).

[13] G. K. Dimitrakakis, E. Tylianakis, and G. E. Froudakis, "Pillared Graphene: A New 3-D Network Nanostructure for Enhanced Hydrogen Storage," Nano Lett. **8**, 3166–3170 (2008).

[14] R. M. Ferullo, N. F. Domancich, and N. J. Castellani, "On the performance of van der Waals corrected-density functional theory in describing the atomic hydrogen physisorption on graphite," Chem. Phys. Lett **500**, 283–286 (2010).

[15] X. Sha and B. Jackson, "First-principles study of the structural and energetic properties of H atoms on a graphite (0001) surface," Surf. Sci. **496**, 318–330 (2002).

[16] L. Jeloaica and V. Sidis, "DFT investigation of the adsorption of atomic hydrogen on a cluster-model graphite surface," Chem. Phys. Lett. **300**, 157–162 (1999).

[17] S. Sahu and G. C. Rout, "Band gap opening in graphene: a short theoretical study," Int. Nano Lett. **7**, 81–89 (2017).

[18] H. González-Herrero, J. M. Gómez-Rodríguez, P. Mallet, M. Moaied, J. J. Palacios, C. Salgado, M. M. Ugeda, J.-Y. Veuillen, F. Yndurain, and I. Brihuega, "Atomic-scale control of graphene magnetism by using hydrogen atoms," Science **352**, 437–441 (2016).

[19] H. González-Herrero, E. C. del Río, P. Mallet, J.-Y. Veuillen, J. J. Palacios, J. M. Gómez-Rodríguez, I. Brihuega, and F. Ynduráin, "Hydrogen physisorption channel on graphene: a highway for atomic H diffusion," 2D Mater. **6**, 021004 (2019).

[20] H. González-Herrero, E. C. del Río, P. Mallet, J.-Y. Veuillen, J. J. Palacios, J. M. Gómez-Rodríguez, I. Brihuega, and F. Ynduráin, "Hydrogen physisorption channel on graphene: a highway for atomic H diffusion," 2d Mater. **6**, 021004 (2019).

[21] F. Hummel, T. Tsatsoulis, and A. Grüneis, "Low rank factorization of the Coulomb integrals for periodic coupled cluster theory," J. Chem. Phys. **146**, 124105 (2017).

[22] T. N. Mihm, A. R. McIsaac, and J. J. Shepherd, "An optimized twist angle to find the twist-averaged correlation energy applied to the uniform electron gas," J. Chem. Phys. **150**, 191101 (2019).

[23] J. M. Callahan, M. F. Lange, and T. C. Berkelbach, "Dynamical correlation energy of metals in large basis sets from downfolding and composite approaches," J. Chem. Phys. **154**, 211105 (2021).

[24] G. H. Booth, A. Grüneis, G. Kresse, and A. Alavi, "Towards an exact description of electronic wavefunctions in real solids," Nature **493**, 365–370 (2013).

[25] T. Schäfer, F. Libisch, G. Kresse, and A. Grüneis, "Local embedding of coupled cluster theory into the random phase approximation using plane waves," J. Chem. Phys. **154**, 011101 (2021).

[26] A. Benali, K. Gasperich, K. D. Jordan, T. Applencourt, Y. Luo, M. C. Bennett, J. T. Krogel, L. Shulenburger, P. R. C. Kent, P.-F. Loos, A. Scemama, and M. Caffarel, "Toward a systematic improvement of the fixed-node approximation in diffusion Monte Carlo for solids—A case study in diamond," J. Chem. Phys. **153**, 184111 (2020).

[27] T. Schäfer, B. Ramberger, and G. Kresse, "Quartic scaling mp2 for solids: A highly parallelized algorithm in the plane wave basis," J. Chem. Phys. **146**, 104101 (2017).

[28] W. M. C. Foulkes, L. Mitas, R. J. Needs, and G. Rajagopal, "Quantum monte carlo simulations of solids," Rev. Mod. Phys. **73**, 33–83 (2001).

[29] J. G. Brandenburg, A. Zen, M. Fitzner, B. Ramberger, G. Kresse, T. Tsatsoulis, A. Grüneis, A. Michaelides, and D. Alfè, "Physisorption of water on graphene: Subchemical accuracy from many-body electronic structure methods," J. Phys. Chem. Lett. **10**, 358–368 (2019).

[30] J. P. Perdew, K. Burke, and M. Ernzerhof, "Generalized Gradient Approximation Made Simple," Phys. Rev. Lett. **77**, 3865–3868 (1996).

[31] J. P. Perdew, "Unified theory of exchange and correlation beyond the local density approximation," in *Electronic Structure of Solids '91*, Physical Research, Vol. 17, edited by P. Ziesche and H. Eschrig (Akademie Verlag, Berlin, 1991) pp. 11–20.

[32] T. Roman, W. A. Diño, H. Nakanishi, H. Kasai, T. Sugimoto, and K. Tange, "Hydrogen pairing on graphene," Carbon **45**, 218–220 (2007).

[33] Ž. Šljivančanin, E. Rauls, L. Hornekær, W. Xu, F. Besenbacher, and B. Hammer, "Extended atomic hydrogen dimer configurations on the graphite(0001) surface," J. Chem. Phys. **131**, 084706 (2009).

[34] P. O. Lehtinen, A. S. Foster, Y. Ma, A. V. Krasheninnikov, and R. M. Nieminen, "Irradiation-induced magnetism in graphite: A density functional study," Phys. Rev. Lett. **93**, 187202 (2004).

[35] Y. Lin, F. Ding, and B. I. Yakobson, "Hydrogen storage by spillover on graphene as a phase nucleation process," Phys. Rev. B **78**, 041402 (2008).

[36] S. Casolo, O. M. Løvvik, R. Martinazzo, and G. F. Tantardini, "Understanding adsorption of hydrogen atoms on graphene," J. Chem. Phys. **130**, 054704 (2009).

[37] R. H. Miwa, T. B. Martins, and A. Fazzio, "Hydrogen adsorption on boron doped graphene: an ab initio study," Nanotechnology **19**, 155708 (2008).

[38] A. Ishii, M. Yamamoto, H. Asano, and K. Fujiwara, "DFT calculation for adatom adsorption on graphene sheet as a prototype of carbon nanotube functionalization," J. Phys. Conf. Ser. **100**, 052087 (2008).

[39] W. Li, M. Zhao, T. He, C. Song, X. Lin, X. Liu, Y. Xia, and L. Mei, "Concentration dependent magnetism induced by hydrogen adsorption on graphene and single walled carbon nanotubes," J. Magn. Magn. Mater. **322**, 838–843 (2010).

[40] D. W. Boukhvalov, M. I. Katsnelson, and A. I. Lichtenstein, "Hydrogen on graphene: Electronic structure, total energy, structural distortions and magnetism from first-principles calculations," Phys. Rev. B **77**, 035427 (2008).

[41] M. A. Kim, D. C. Sorescu, S. Amemiya, K. D. Jordan, and H. Liu, "Real-time modulation of hydrogen evolution activity of graphene electrodes using mechanical strain," ACS Applied Materials & Interfaces **14**, 10691–10700 (2022).

[42]S. Grimme, J. Antony, S. Ehrlich, and H. Krieg, "A consistent and accurate ab initio parametrization of density functional dispersion correction (DFT-D) for the 94 elements H-Pu," J. Chem. Phys. **132**, 154104 (2010).
[43]A. Annaberdiyev, G. Wang, C. A. Melton, M. C. Bennett, L. Shulenburger, and L. Mitas, "A new generation of effective core potentials from correlated calculations: 3d transition metal series," J. Chem. Phys. **149**, 134108 (2018).
[44]M. C. Bennett, C. A. Melton, A. Annaberdiyev, G. Wang, L. Shulenburger, and L. Mitas, "A new generation of effective core potentials for correlated calculations," J. Chem. Phys. **147**, 224106 (2017).
[45]H. J. Monkhorst and J. D. Pack, "Special points for Brillouin-zone integrations," Phys. Rev. B **13**, 5188–5192 (1976).
[46]N. Marzari, D. Vanderbilt, A. De Vita, and M. C. Payne, "Thermal Contraction and Disordering of the Al(110) Surface," Phys. Rev. Lett. **82**, 3296–3299 (1999).
[47]C. Adamo and V. Barone, "Toward reliable density functional methods without adjustable parameters: The PBE0 model," J. Chem. Phys. **110**, 6158–6170 (1999).
[48]A. V. Krukau, O. A. Vydrov, A. F. Izmaylov, and G. E. Scuseria, "Influence of the exchange screening parameter on the performance of screened hybrid functionals," J. Chem. Phys. **125**, 224106 (2006).
[49]M. F. Peintinger, D. V. Oliveira, and T. Bredow, "Consistent gaussian basis sets of triple-zeta valence with polarization quality for solid-state calculations," J. Comput. Chem. **34**, 451–459 (2012).
[50]H. Kruse and S. Grimme, "A geometrical correction for the inter- and intra-molecular basis set superposition error in Hartree-Fock and density functional theory calculations for large systems," J. Chem. Phys. **136**, 154101 (2012).
[51]J. G. Brandenburg, M. Alessio, B. Civalleri, M. F. Peintinger, T. Bredow, and S. Grimme, "Geometrical Correction for the Inter- and Intramolecular Basis Set Superposition Error in Periodic Density Functional Theory Calculations," J. Phys. Chem. A **117**, 9282–9292 (2013).
[52]P. Giannozzi, O. Baseggio, P. Bonfà, D. Brunato, R. Car, I. Carnimeo, C. Cavazzoni, S. de Gironcoli, P. Delugas, F. Ferrari Ruffino, A. Ferretti, N. Marzari, I. Timrov, A. Urru, and S. Baroni, "Quantum ESPRESSO toward the exascale," J. Chem. Phys. **152**, 154105 (2020).
[53]P. Giannozzi, S. Baroni, N. Bonini, M. Calandra, R. Car, C. Cavazzoni, D. Ceresoli, G. L. Chiarotti, M. Cococcioni, I. Dabo, A. Dal Corso, S. de Gironcoli, S. Fabris, G. Fratesi, R. Gebauer, U. Gerstmann, C. Gougoussis, A. Kokalj, M. Lazzeri, L. Martin-Samos, N. Marzari, F. Mauri, R. Mazzarello, S. Paolini, A. Pasquarello, L. Paulatto, C. Sbraccia, S. Scandolo, G. Sclauzero, A. P. Seitsonen, A. Smogunov, P. Umari, and R. M. Wentzcovitch, "QUANTUM ESPRESSO: a modular and open-source software project for quantum simulations of materials," J. Phys.: Condens. Matter **21**, 395502 (19pp) (2009).
[54]P. Giannozzi, O. Andreussi, T. Brumme, O. Bunau, M. B. Nardelli, M. Calandra, R. Car, C. Cavazzoni, D. Ceresoli, M. Cococcioni, N. Colonna, I. Carnimeo, A. D. Corso, S. de Gironcoli, P. Delugas, R. A. D. Jr, A. Ferretti, A. Floris, G. Fratesi, G. Fugallo, R. Gebauer, U. Gerstmann, F. Giustino, T. Gorni, J. Jia, M. Kawamura, H.-Y. Ko, A. Kokalj, E. Küçükbenli, M. Lazzeri, M. Marsili, N. Marzari, F. Mauri, N. L. Nguyen, H.-V. Nguyen, A. O. de-la Roza, L. Paulatto, S. Poncé, D. Rocca, R. Sabatini, B. Santra, M. Schlipf, A. P. Seitsonen, A. Smogunov, I. Timrov, T. Thonhauser, P. Umari, N. Vast, X. Wu, and S. Baroni, "Advanced capabilities for materials modelling with QUANTUM ESPRESSO," J. Phys.: Condens. Matter **29**, 465901 (2017).
[55]R. Dovesi, A. Erba, R. Orlando, C. M. Zicovich-Wilson, B. Civalleri, L. Maschio, M. Rérat, S. Casassa, J. Baima, S. Salustro, and B. Kirtman, "Quantum-mechanical condensed matter simulations with CRYSTAL," Wiley Interdiscip. Rev. Comput. Mol. Sci **8**, e1360 (2018).
[56]R. Dovesi, F. Pascale, B. Civalleri, K. Doll, N. M. Harrison, I. Bush, P. D'Arco, Y. Noël, M. Rérat, P. Carbonnière, M. Causà, S. Salustro, V. Lacivita, B. Kirtman, A. M. Ferrari, F. S. Gentile, J. Baima, M. Ferrero, R. Demichelis, and M. De La Pierre, "The CRYSTAL code, 1976–2020 and beyond, a long story," J. Chem. Phys. **152**, 204111 (2020).
[57]E. Aprà, E. J. Bylaska, W. A. de Jong, N. Govind, K. Kowalski, T. P. Straatsma, M. Valiev, H. J. J. van Dam, Y. Alexeev, J. Anchell, V. Anisimov, F. W. Aquino, R. Atta-Fynn, J. Autschbach, N. P. Bauman, J. C. Becca, D. E. Bernholdt, K. Bhaskaran-Nair, S. Bogatko, P. Borowski, J. Boschen, J. Brabec, A. Bruner, E. Cauët, Y. Chen, G. N. Chuev, C. J. Cramer, J. Daily, M. J. O. Deegan, T. H. Dunning, M. Dupuis, K. G. Dyall, G. I. Fann, S. A. Fischer, A. Fonari, H. Fr uchtl, L. Gagliardi, J. Garza, N. Gawande, S. Ghosh, K. Glaesemann, A. W. Götz, J. Hammond, V. Helms, E. D. Hermes, K. Hirao, S. Hirata, M. Jacquelin, L. Jensen, B. G. Johnson, H. Jónsson, R. A. Kendall, M. Klemm, R. Kobayashi, V. Konkov, S. Krishnamoorthy, M. Krishnan, Z. Lin, R. D. Lins, R. J. Littlefield, A. J. Logsdail, K. Lopata, W. Ma, A. V. Marenich, J. Martin del Campo, D. Mejia-Rodriguez, J. E. Moore, J. M. Mullin, T. Nakajima, D. R. Nascimento, J. A. Nichols, P. J. Nichols, J. Nieplocha, A. Otero-de-la Roza, B. Palmer, A. Panyala, T. Pirojsirikul, B. Peng, R. Peverati, J. Pittner, L. Pollack, R. M. Richard, P. Sadayappan, G. C. Schatz, W. A. Shelton, D. W. Silverstein, D. M. A. Smith, T. A. Soares, D. Song, M. Swart, H. L. Taylor, G. S. Thomas, V. Tipparaju, D. G. Truhlar, K. Tsemekhman, T. Van Voorhis, A. Vázquez-Mayagoitia, P. Verma, O. Villa, A. Vishnu, K. D. Vogiatzis, D. Wang, J. H. Weare, M. J. Williamson, T. L. Windus, K. Woliński, A. T. Wong, Q. Wu, C. Yang, Q. Yu, M. Zacharias, Z. Zhang, Y. Zhao, and R. J. Harrison, "NWChem: Past, present, and future," J. Chem. Phys. **152**, 184102 (2020).
[58]J. B. Anderson, "Quantum chemistry by random walk: Higher accuracy," J. Chem. Phys. **73**, 3897–3899 (1980).
[59]K. Esler, J. Kim, D. Ceperley, and L. Shulenburger, "Accelerating quantum monte carlo simulations of real materials on gpu clusters," Computing in Science Engineering **14**, 40–51 (2012).
[60]N. D. Drummond, M. D. Towler, and R. J. Needs, "Jastrow correlation factor for atoms, molecules, and solids," Phys. Rev. B **70**, 235119 (2004).
[61]C. J. Umrigar, J. Toulouse, C. Filippi, S. Sorella, and R. G. Hennig, "Alleviation of the Fermion-Sign Problem by Optimization of Many-Body Wave Functions," Phys. Rev. Lett. **98**, 110201 (2007).
[62]A. Zen, J. G. Brandenburg, A. Michaelides, and D. Alfè, "A new scheme for fixed node diffusion quantum Monte Carlo with pseudopotentials: Improving reproducibility and reducing the trial-wave-function bias," J. Chem. Phys. **151**, 134105 (2019).
[63]M. Casula, S. Moroni, S. Sorella, and C. Filippi, "Size-consistent variational approaches to nonlocal pseudopotentials: Standard and lattice regularized diffusion Monte Carlo methods revisited," J. Chem. Phys. **132**, 154113 (2010).
[64]C. Lin, F. H. Zong, and D. M. Ceperley, "Twist-averaged boundary conditions in continuum quantum monte carlo algorithms," Phys. Rev. E **64**, 016702 (2001).
[65]A. Zen, S. Sorella, M. J. Gillan, A. Michaelides, and D. Alfè, "Boosting the accuracy and speed of quantum Monte Carlo: Size consistency and time step," Phys. Rev. B **93**, 241118 (2016).
[66]H. Shin, Y. Luo, A. Benali, and Y. Kwon, "Diffusion Monte Carlo study of O_2 adsorption on single layer graphene," Phys. Rev. B **100**, 075430 (2019).
[67]D. Cortés-Arriagada, S. Gutiérrez-Oliva, B. Herrera, K. Soto, and A. Toro-Labbé, "The mechanism of chemisorption of hydrogen atom on graphene: Insights from the reaction force and reaction electronic flux," J. Chem. Phys. **141**, 134701 (2014).
[68]H. Jiang, M. Kammler, F. Ding, Y. Dorenkamp, F. R. Manby, A. M. Wodtke, T. F. Miller, A. Kandratsenka, and O. Bünermann, "Imaging covalent bond formation by H atom scattering from graphene," Science **364**, 379–382 (2019).

[69] J. Kim, A. D. Baczewski, T. D. Beaudet, A. Benali, M. C. Bennett, M. A. Berrill, N. S. Blunt, E. J. L. Borda, M. Casula, D. M. Ceperley, S. Chiesa, B. K. Clark, R. C. Clay, K. T. Delaney, M. Dewing, K. P. Esler, H. Hao, O. Heinonen, P. R. C. Kent, J. T. Krogel, I. Kylänpää, Y. W. Li, M. G. Lopez, Y. Luo, F. D. Malone, R. M. Martin, A. Mathuriya, J. McMinis, C. A. Melton, L. Mitas, M. A. Morales, E. Neuscamman, W. D. Parker, S. D. P. Flores, N. A. Romero, B. M. Rubenstein, J. A. R. Shea, H. Shin, L. Shulenburger, A. F. Tillack, J. P. Townsend, N. M. Tubman, B. V. D. Goetz, J. E. Vincent, D. C. Yang, Y. Yang, S. Zhang, and L. Zhao, "QMCPACK: an open source ab initio quantum Monte Carlo package for the electronic structure of atoms, molecules and solids," J. Phys.: Condens. Matter **30**, 195901 (2018).

[70] P. R. C. Kent, A. Annaberdiyev, A. Benali, M. C. Bennett, E. J. Landinez Borda, P. Doak, H. Hao, K. D. Jordan, J. T. Krogel, I. Kylänpää, J. Lee, Y. Luo, F. D. Malone, C. A. Melton, L. Mitas, M. A. Morales, E. Neuscamman, F. A. Reboredo, B. Rubenstein, K. Saritas, S. Upadhyay, G. Wang, S. Zhang, and L. Zhao, "QMCPACK: Advances in the development, efficiency, and application of auxiliary field and real-space variational and diffusion quantum Monte Carlo," J. Chem. Phys. **152**, 174105 (2020).

[71] J. T. Krogel, "Nexus: A modular workflow management system for quantum simulation codes," Comput. Phys. Commun. **198**, 154–168 (2016).

[72] J. D. Hunter, "Matplotlib: A 2d graphics environment," Computing in Science & Engineering **9**, 90–95 (2007).

[73] K. Momma and F. Izumi, "*VESTA3* for three-dimensional visualization of crystal, volumetric and morphology data," J. Appl. Crystallogr. **44**, 1272–1276 (2011).